A THREE-COMPONENT MODEL FOR THE ASSESSMENT OF THE IMPACT OF HIGH-CO_2 LEVELS AND ITS APPLICATION IN PORTUGAL

R. J. AGUIAR

LNETI — Departamento de Energias Renováveis
Estrada do Paço do Lumiar, 1699 Lisboa Codex

AND

F. D. SANTOS

Instituto Nacional de Meteorologia e Geofísica
Rua C. do Aeroporto de Lisboa, 1700 Lisboa
Portugal

(Received 30 May 1988)

ABSTRACT — A simple model is described which enables preliminary studies of the impact in Portugal of the release of large quantities of carbon dioxide to the atmosphere, due to man-related activities. The model assembles three separate previous models for i) the carbon cycle, ii) the climate system and iii) the biosphere response. Calibration and sensitivity studies are done and the results yielded by the model with suitable (conservative) estimates on the CO_2 future release leads to the identification of temperature as the main factor influencing the distribution of the bioclimatic regions in Portugal and indicates a significative impact on its biosphere, namely in the appearance of predesertification areas.

1 — INTRODUCTION

The continuous and increasing release of carbon dioxide into the atmosphere since the Industrial Revolution, due to growing industrial and agricultural activities, tends to disrupt the natural equilibrium of the CO_2 reservoirs existing on Earth.

As a consequence, it is calculated [1] that about 56 % of the CO_2 released by mankind remains in the atmosphere, leading to an enhanced greenhouse effect. The predicted rise in the average temperatures may have several important consequences on the

Earth's climate system: melting of ice covers, rise in sea levels, modifications in the general atmospheric circulation, namely in the hidrological cycle, and in the oceanic movements.

In principle, the higher CO_2 levels would also increase the productivity of the biosphere. However, detailed models are necessary, in view of the complexity of the carbon cycle and of the atmospheric circulation and also in view of the variety of responses of different plants to the conditions of temperature, soil, available radiation and available moisture.

Three areas of modelling can then be distinguished, where: i) models deal with the carbon cycle, using a CO_2 input based on some kind of economic scenario; ii) models simulate the general circulation of the atmosphere, in a way similar to the meteorological prediction models, and iii) models simulate the response of plants to different environmental conditions. In the order depicted above, each level of simulation should use the results of the anterior level, enabling then the computation of a global time response of the climate/biosphere system. However, this is seldom done in current literature.

In the present work, simplified models for the three aspects mentioned above are applied for the particular case of Portugal. Comparison is made of the results obtained with i) average past meteorological conditions and ii) meteorological conditions predicted by the model, assuming a conservative estimate for the future consumption of fossil fuels and deforestation. This will permit a first assessment of the impact on Portugal of high atmospheric-CO_2 levels.

2 — MODELLING THE CO_2 CYCLE

2.1 — *Description of the model*

The four main reservoirs of carbon on Earth are the sedimentary rocks, the oceans, the biosphere and the atmosphere. The CO_2 cycle model does not include the first reservoir, because it is known that the estimated fluxes from and to the sediments are only about 10^{-3} to 10^{-4} of the atmospheric carbon mass per year.

On the other hand, the oceanic reservoir is splitted in a superficial (mixed) layer and a deep layer, accounting in this

simplified way for the convection, diffusion and mixing processes that occur in the ocean.

Thus, the CO_2-cycle model consists of four reservoirs, connected by fluxes with each other as shown in Fig. 1. The dynamic equilibrium existing in this system is perturbed by two fluxes representing human activities: a deforestation flux and a fossil combustible flux.

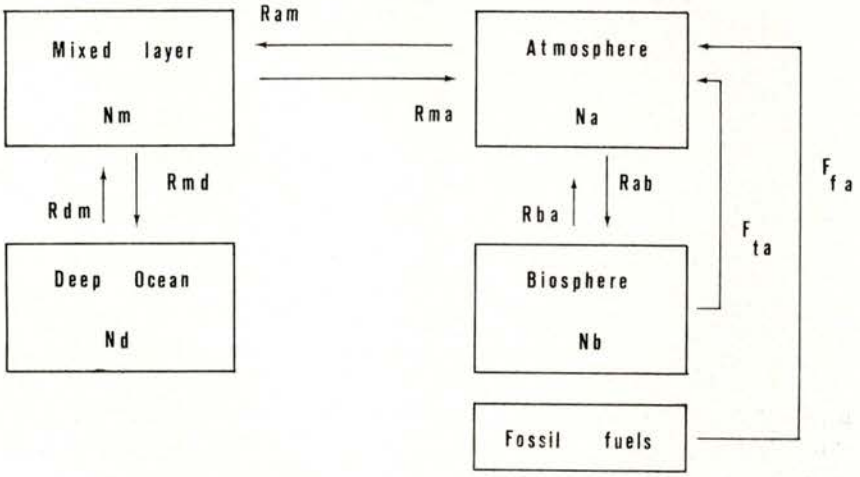

Fig. 1 — Box model for the CO_2 cycle.

It is worthwhile to note that the fossil organic matter reserves, i. e. carbon, oil and natural gas, are considered to be part of the biosphere; however, since they do not interact with other reservoirs in any way except by the man-induced flux, their mass must not be taken into account for describing the biosphere's behaviour.

The fluxes R_{ij} between carbon reservoirs with contents N_i are described by linear expressions, as follows:

$$R_{ij} = K_{ij} \times N_i \qquad (1)$$

where the K_{ij} are inverses of residence times for atoms of carbon transiting from reservoir i to reservoir j. These indexes can take the values i, j = a, b, m, d for atmosphere, biosphere, mixed and deep ocean layers, respectively.

However, since the transfer of carbon to the biosphere should depend in some way on the mass of the biosphere itself and since upper limits to growth are known to exist (eg. water, nutrient and radiation availabilities), an exception must be made for R_{ab}, in which case a logarithmic form [1] was chosen:

$$R_{ab} = K_{ab}\ (N_{ao}\ (1 + e\ \mathrm{Ln}(N_a / N_{ao}))). \qquad (2)$$

Here, N_{ao} is the pre-industrial atmospheric content of CO_2 and e is a biotic growth factor, accounting for the fertilizing effect of carbon dioxide on the biosphere.

Tests with various forms for the deforestation and fossil fuel consumption (eg. linear, logarithmic, exponencial) [2] and comparison with observed data on CO_2 atmospheric levels [1] indicate that realistic behaviour of the model is possible when a logistic form is taken for both fluxes:

$$F_{ia}(t) = U / (1 + \exp\{4B(t_m - t) / U_i\}) \quad i = f, t \qquad (3)$$

where f stands for fossil fuel consuption (t for deforestation), U is the pre-industrial total content in carbon of the known economically exploitable reserves (terrestrial living biomass) and B is the maximum production rate (deforestation rate), taking place at time $t = t_m$.

The complete set of differential equations describing the CO_2-cycle model will be then

$$\begin{aligned}
dN_b/dt &= -K_{ba}\ N_b(t) + R_{ab} - F_{ta}(t) \\
dN_m/dt &= K_{am}\ N_a(t) + N_{dm}\ N_d(t) - K_{ma}\ N_m(t) - \\
&\quad - K_{md}\ N_m(t) \\
dN_d/dt &= K_{md}\ N_m(t) - K_{dm}\ N_d(t) \\
dN_a/dt &= -K_{am}\ N_a(t) + K_{ba}\ N_b(t) + K_{ma}\ N_m(t) - \\
&\quad - R_{ab} + F_{fa}(t) + F_{ta}(t)
\end{aligned} \qquad (4)$$

with R_{ab}, F_{fa} and F_{ta} given by expression (2) and (3).

2.2 — *Calibration of the CO_2-cycle model*

With the anthropogenic fluxes set to zero, and assuming a linear form for R_{ab}, the set of equations (4) can be written in a

matricial form, $dN/dt = AN$. it can be shown that a equilibrium state exists, the one that corresponds to the eigenvalue zero of the matrix of coefficients A. The corresponding eigenvector, normalized by the atmospheric carbon content [2, 3], is $\{1, K_{ab}/K_{ab}, K_{am}/K_{ma}, (K_{am}\ K_{md})/K_{ma}\ K_{dm})\}$. Once estimates are known for the interaction constants K_{ij} and contents N_i (see for instance [1, 3]), it is possible to adjust them consistently with the stationary state eigenvector. The values found for the present model are listed in Table I.

TABLE I — Numerical constants used in the CO_2-cycle model

Reservoir content in 1975 (10^{12} Kg C)	Interaction constants (year^{-1})
$N_a = 710$	$K_{ab} = 1/21.57$ $K_{ba} = 1/28.60$
$N_b = 815$	$K_{am} = 1/6.30$ $K_{ma} = 1/7.36$
$N_m = 815$	$K_{md} = 1/33.12$ $K_{dm} = 1/16.00$
$N_d = 42000$	

Pre-industrial atmospheric CO_2: $N_{ao} = 630 \times 10^{12}$ Kg C
Biotic growth factor: $e = 0.5$

For the man-induced fluxes, values of maximum rates B and corresponding times of ocurrence t_m were adjusted so that the model would fit to past trends; the values obtained are presented in Table II.

TABLE II — Numerical values for the logistic fluxes of deforestation and fossil fuel consumption

	U (10^{12} Kg C)	B (10^{12} Kg C year^{-1})	t_m
World forests:	835	9	2000
Fossil reserves:	4400	40	2070

Fig. 2 represents the predicted evolution of carbon content for the biosphere and atmosphere, according to this model, integrated with a standard Runge-Kutta method.

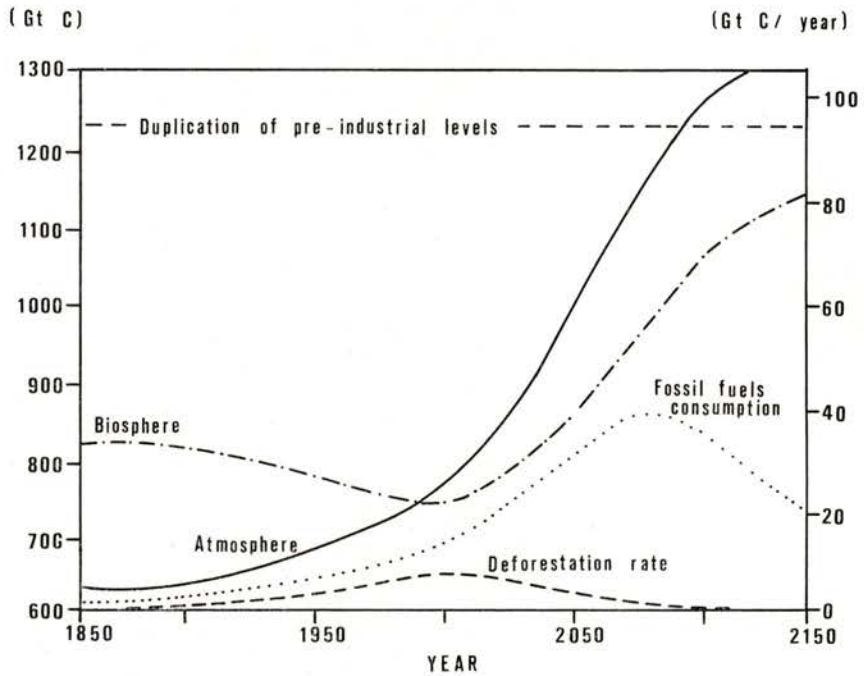

Fig. 2 — Evolution of carbon content of atmosphere and biosphere under logistic deforestation and fossil fuel consumption.

3 — VERTICAL ONE-DIMENSIONAL ATMOSPHERIC MODEL

3.1 — *Thermodinamic structure of the atmosphere*

A radiative-convective type atmospheric model is chosen in view of its relative simplicity for implementation and of the good agreement this class of models shows with more complex ones, as the GCM's (tridimensional global circulation models). In the radiative-convective models, the (unidimensional) structure of the atmosphere for average conditions is evaluated considering the equilibrium between the radiative flux and a parametrized con-

vective heat flux; the temperature profile is adjusted to be less or equal to the «stable» thermal gradient of 6.5 K/Km.

The model of Weare and Snell (1974) is chosen as it gives a more complete treatment of the atmosphere than others, both because its analytical description seems superior to the use of discrete levels or of a standard atmosphere and because it introduces a parametrization for clouds and precipitation processes [5] (instead of a fixed cloudiness).

Consider first the thermodinamic equilibrium of a vertical column of atmosphere standing over a plane surface representing Hidrosphere, Litosphere and Criosphere. A particle of humid air suffers a quasi-static expansion and rises through a stable environment, mantaining the equilibrium in the gravitational field. Using essentially the law for ideal gases, the geostrophic equilibrium aproximation and the Clapeyron-Clausis equation it is possible [2] to derive equations for the particle temperature and water content dependence on the height z:

$$\frac{\partial T}{\partial z} = - \frac{\left(1 + \frac{n_{2A}(z)\ \Delta H_i}{n_1\ R\ T(z)}\right)\left(1 + \frac{n_{2B}(z)}{n_A(z)}\right) M(z)\ g}{C + C_B \frac{n_{2B}(z)}{n_A(z)} - \frac{A}{n_A(z)} + \frac{n_{2A}(z)\ \Delta H_i^2}{n_1\ R\ T^2(z)}} \tag{5a}$$

$$\frac{\partial n_{2A}}{\partial z} = - \frac{n_A \left(C - \frac{\Delta H_i}{T(z)} + n_{2B}(z)\ C_B - A\right)}{\frac{n_1\ R\ T(z)}{n_{2A}(z)} + \Delta H_i} \tag{5b}$$

where:

- M = average molecular mass of humid air
- g = acceleration of gravity (9.8 m s^{-2})
- R = universal constant for ideal gases
- A = parameter for the convective transfer of entropy
- T = temperature
- C = average specific heat for the mixture air-water vapour
- C_B = specific heat for condensed water
- n = number of moles of component j
- ΔH_i = latent heat for: i = 1 — vapour/liquid transition; i = 2 — vapour/ice transition

and where quantities related with various components are indexed with

j = 1 for dry air,
j = 2A for water vapour,
j = 2B for condensed water (liquid and/or solid).

Under the condition of water conservation, the water condensed in a rise of δz is

$$\delta n_{2B} = - \frac{\partial n_{2A}(z)}{\partial T(z)} \frac{\partial T(z)}{\partial z} \delta z . \qquad (5c)$$

It is admited that only a very small fraction of the condensed water, 1 - f, remains in the particle, in the liquid form if $T(z) > 273.15$ K, and in the solid state otherwise. The remaining fraction, f, falls to the surface. In this way the existence of clouds and precipitation in the atmosphere is accounted for.

The set of partial differencial equations (5) was solved with a Euler method and vertical steps of one meter, with the averaged (annual, global) boundary conditions $T(0) = 288$ K, $n_{2B}(0) = 0$ and a value for $n_{2A}(0)$ deduced from a surface average pressure of $P(0) = 1013$ hPa and a relative humidity of $U(0) = 0.75$.

The atmosphere was found to be stable (i. e. thermal gradient less or equal to 6.5 K/Km) when $A = -14.5$ J/mol K. The value of f that yielded average total precipitable water compatible with actual conditions was f = 99.589 %. The vertical distribution of temperature, water vapour and density of condensed water for a set of surface temperatures are representd in Figs. 3 through 5.

While temperature and water vapour seem to follow a realistic pattern, it is clear that no cloud has the vertical extent and the vertical distribution of water shown in Fig. 5. However, note that this «diffuse» cloud is not a model of real clouds, but rather a representation of average conditions of clear and overcaste skies throughout the year.

3.2 — *Particulate constitution of clouds*

The distribution of condensed water in the form of droplets or ice cristals (depending on temperature) is assumed to be given

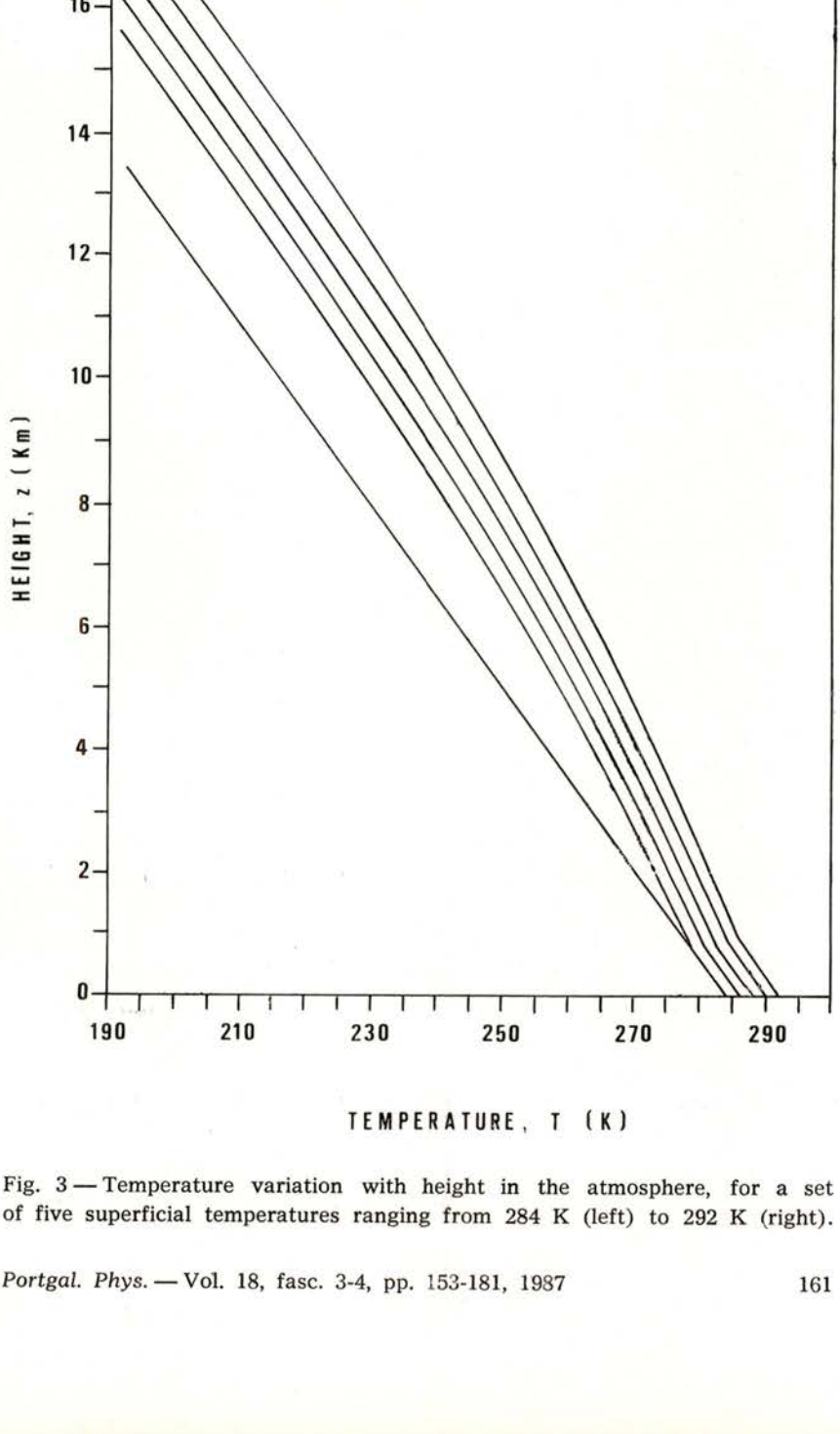

Fig. 3 — Temperature variation with height in the atmosphere, for a set of five superficial temperatures ranging from 284 K (left) to 292 K (right).

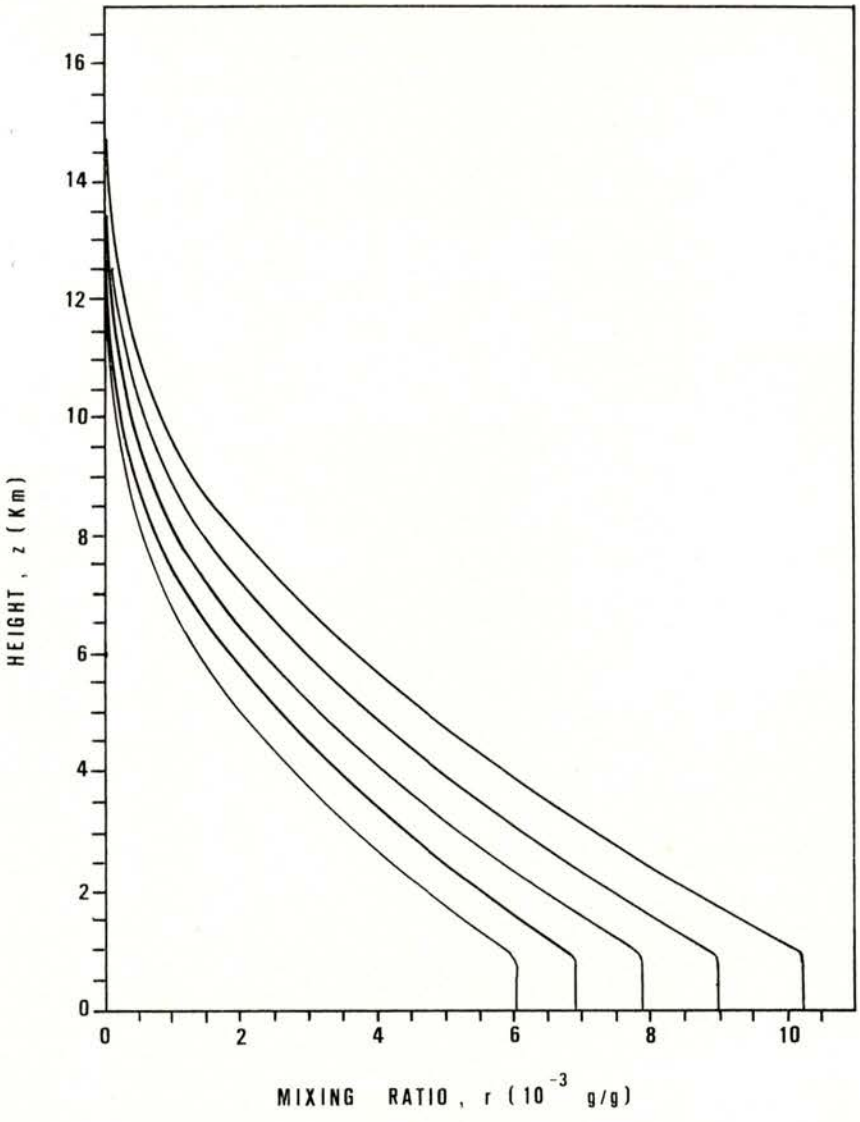

Fig. 4 — The same as in Fig. 3, for water vapour content.

by a size-distribution law similar to that used by Deirmendjian (1964)

$$n(r) = ar^{\alpha} \exp(-br^{\gamma}) \qquad (6a)$$

where n (r) is the volumic concentration of particles — assumed sphearical — with radius r. The constant a is related with the

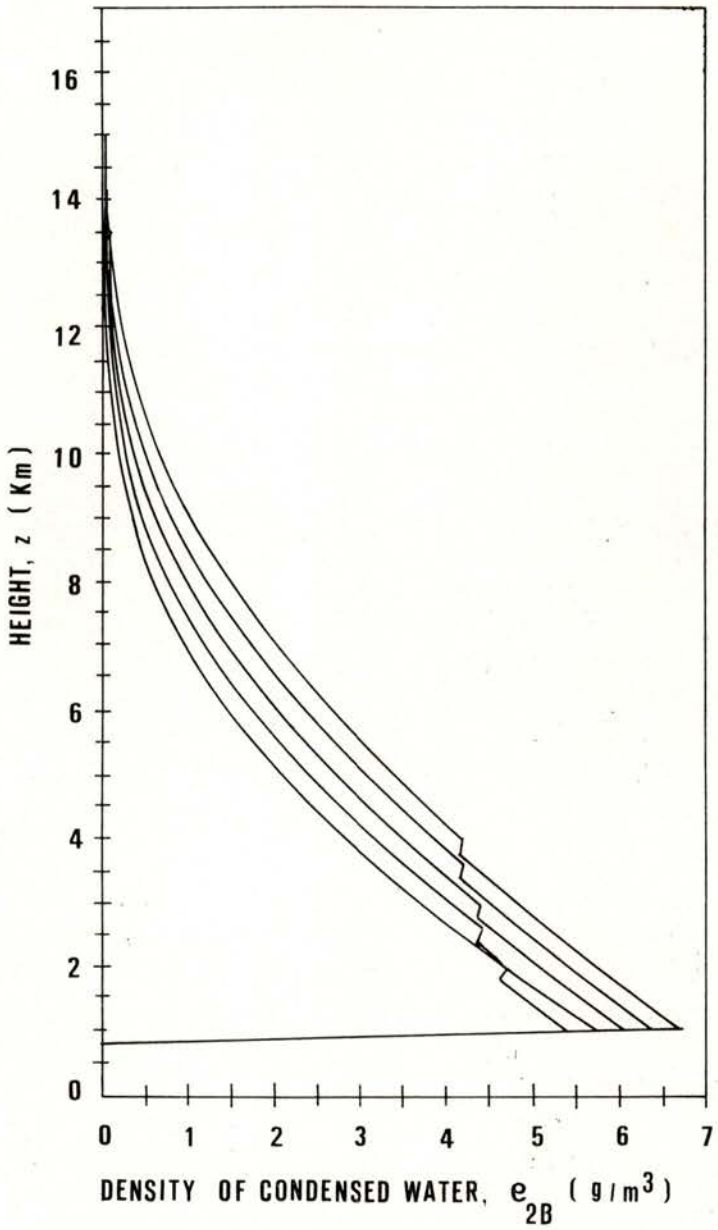

Fig. 5 — The same as in Fig. 3, for condensed water content.

total number of particules per unit volume and b to a modal droplet radius, $r = 4\ \mu m$. The positive constants α and γ can be fitted so that the function n (r) will follow the experimental distributions for cumulus clouds, yielding $\alpha = 6$, $\gamma = 1$. Generalizing n (r) to n (r, z), for each level z, it is possible to relate a (z) to the condensed water volumic mass ρ_{2B} (z) :

$$n(r, z) = \frac{3 \times 1.5^{10}\ r_2}{4 \times 9!\ \pi \rho}\ \rho_{2B}(z)\ r^6\ \exp\{-1.5\ r\}\ \mu m\ m^{-3} \quad (6b)$$

Here ρ is the volumic mass of the droplets, $r_2 = 12\ \mu m$ is a superior limit to the particle radius and both ρ_{2B} and ρ are expressed in g/m^3.

3.3 – *Downward radiative flux*

The analytic solution derived by Sagan and Pollock (1967) for the radiative transfer equation of Chandrasekar in the case of a plane-stratified atmosphere is used. Some assumptions for this solution are i) anisotropic non-conservative diffusion occurs because of the dielectric particles suspended in the atmosphere ii) Mie theory is valid (particle size much smaller than radiation wavelenght) iii) the Schuster-Schwartschild two-flux aproximation, modified by the use of an assimetry factor B (see Fig. 6), is

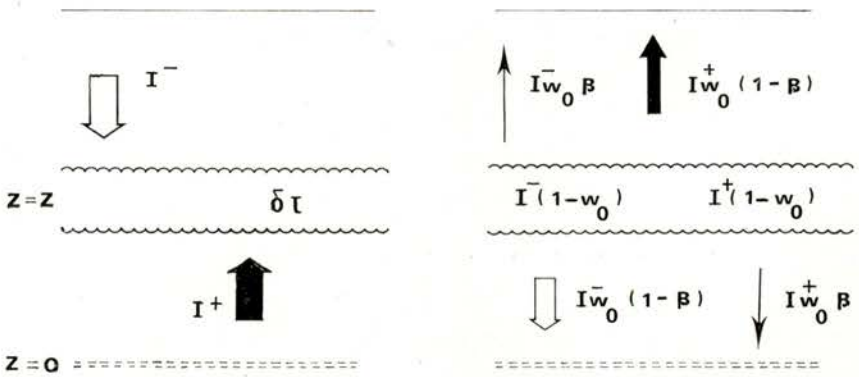

Fig. 6 — Scheme of the two-flux approximation (for visible radiation).

assumed. With the boundary condition $t(\tau) = 1$ for a null optical depth $\tau = 0$, the fractions of absorbed, a, reflected, r and transmited energy by the atmosphere, t, can be written [7]:

$$a = 1 - r - t \tag{7a}$$

$$r = \frac{(u+1)\ (u-1)\ (\exp\{\tau'\} - \exp\{-\tau'\})}{(u+1)^2\ \exp\{\tau'\} - (u-1)^2\ \exp\{-\tau'\}} \tag{7b}$$

$$t = \frac{4u}{(u+1)^2\ \exp\{\tau'\} - (u-1)^2\ \exp\{-\tau'\}} \tag{7c}$$

where $u = (1 - w_0 + 2Bw_0)/(1 - w_0)$ and $\tau' = \sqrt{3}\ u\ (1 - w_0)\ \tau$. The parameter w_0 is called the albedo for single diffusion and takes the values $w_0 = 0.999$ for water and $w_0 = 0.95$ for aerosols. Also, the assimetry factor is $B = 0.078$ and $B = 0.18$ for water and for aerossols respectively.

For the aerosols a value of $\tau = 0.1$ is assumed. The determination of τ for the case of water is somewhat complicated. Using experimental data for the extintion coefficients in the case of water droplets [8] and the Planck equation for the spectral energy density, a very simple relation could be obtained [2] with the help of numerical integrations:

$$\tau(z) = 0.074815\ W(z) \tag{8}$$

where W (z) is the water content of the cloud from its base to level z.

Since the reflectivity R_{AB} of two superposed layers A and B overlying a plane surface of refllectivity r_C can be given by [5]

$$R_{AB} = r_A + \frac{t_A^2\ [r_C t_B^2 + r_B(1 - r_B r_C)]}{(1 - r_B r_C)\ (1 - r_A r_B) - r_A r_C t_B^2} \tag{9}$$

the total terrestrial albedo α will be calculated as a simple average between the case of a cloud layer on the top of an aerosol layer and the case corresponding to the inverse situation. The transmissivities and reflectivities of cloud and aerosol are known from the respective optical depths and from the equations (7), but a

parametrization for the ground average reflectivity r_C depending on temperature must be obtained. The empirical equations of Hollin [9] and of Morner [10] are used, giving:

$$\langle\Theta_S\rangle = 65 - 0.1\ [T(O) - 288.] \quad (10a)$$

$$\langle\Theta_N\rangle = 65 - 2.0\ [T(O) - 288.] \quad (10b)$$

$$\langle\Theta\rangle = (\langle\Theta_N\rangle + \langle\Theta_S\rangle)/2 \quad (10c)$$

$$r_C = (1 - \sin\ (\langle\Theta\rangle))\ r_i + \sin\ (\langle\Theta\rangle)\ r_o \quad (11)$$

where the equations (10a, b) correspond to the amplitudes Θ, in degrees, of the southern and northern ice caps, respectively. In equation (11) the reflectivity of ice r_i and of a weighted average of other surfaces (including ocean water) r_0 are given by $r_i = 0.60$ and $r_0 = 0.07$.

3.4 — *Upward radiative flux*

In this section the infrared radiation absorption is modelled for the main absorbers in the atmosphere: water, carbon dioxide and ozone. The approach of Rodgers [11, 12], which avoids the integrations through the complicated spectrum lines, is followed. An emissivity function ε is parametrized: for the whole spectrum in the case of water; of the 667 cm^{-1} band in the case of CO_2.

The upward radiation flux at level z, F (z), can be written

$$F(z) - F(O) = \int_0^{U(z)} (B(u) - B(U))\ (d\varepsilon / du)\ du \quad (12a)$$

where B stands for the total Planck function, i. e. B_ν for each wave number ν integrated over all the wave numbers. An integration in altitude was substituted in Eq. 12a by an integration over total absorber quantities u, from the surface up to the height z, using the formula [12]:

$$u(z, 0) = 1.66\ (M_1/R) \int_z^0 (r_B(z)/T(z))\ P^2(z)\ \exp\ [\beta(T(z) - 250)]\ dz \quad (12b)$$

which includes the correction due to the variation of absorption with temperature (exponencial term with $\beta = 0.005$) and Elssasser's factor 1.66 to account for integration over all zenithal angles. In Eq. 12b, P stands for pressure, M_1 for molecular mass of dry air and r_B for mixing ratio of the condensed water. The definition and parametrization of water emissivity ε is as follows:

$$\varepsilon = \int_0^{\infty} A_\nu \, (dB/dB_\nu) \, d\nu_\nu = \begin{cases} \sum_{n=1}^{N} a_n \, u^2 & u < v \\ \sum_{n=0}^{N} b_n \, (\log u) & u \geqslant v \end{cases} \quad (12c)$$

where A is the absorvity at wave number ν (see Table III for the numerical values of constants a_n and b_n).

TABLE III — Numerical constants for water and CO_2 emissivity parametrizations

	H_2O	CO_2		H_2O	CO_2
v	0.001 Kg/m	0.1 atm/cm	b_0	0.5983	74.103
a_1	9.329	160.87	b_1	0.15068	19.632
a_2	— 446.4	— 326.50	b_2	0.034041	0.821
a_3	824.0	— 158.22	b_3	0.0065535	— 0.11834
a_4	259700.	—	b_4	0.0004887	—

This type of calculation differs from most radiative-convective models as it does not consider the clouds to be black bodies for infrared radiation. In fact, in this model there are no massive clouds and clear sky zones but rather a diffuse cloud, as already explained.

For the carbon dioxide, only the emissivity for the strongest band is parametrized: all the radiation absorbed by this gas will be assumed to lay in an interval of 200 cm^{-1}. In this spectral region there is superposition between the absorption bands of water and carbon dioxide.

The transmissivity of the water T_{H_2O} in this region, evaluated with a Goody type randob-line spectrum, was accounted for [11] in the expression for the CO_2 absorbed infrared flux:

$$F_{CO_2}(z) = 200 \left(\int_z^0 B_{667}(z') \; [d(\varepsilon_{CO_2}(z, z') \; T_{H_2O}(z, z'))/dz] \; dz' - B_{667}(0) \; \varepsilon_{CO_2}(z, 0) \; T_{H_2O}(z, 0) \right) \quad (13a)$$

The emissivity ε_{CO_2} is of the same form as discussed for water (see Table III), and

$$T_{H_2O}(z, z') = \exp^{r} - (km/\delta) \; (1 + km/\pi a\phi)^{1/2}] \quad (13b)$$

where m and m/ϕ are quantities similar to u (ie. absorber quantities corrected for temperature effects [2]. The remaining variables, adjusted for the region of interest, take the values $k/\delta = 7.345$ and $k/\pi a = 142.47$, already corrected with Elssasser's factor.

3.5 — *Calibrations and sensitivity study*

Figure 7 shows total, H_2O-related and CO_2-related infrared absorption from the surface, in the model's atmosphere. Comparison of simulated upward radiation flux and satellite measurements indicates some underestimation of this value. The thermodinamic equilibrium of the Earth-Atmosphere system is preserved by adjusting the emissivity of ozone, following Staley and Jurica [13]:

$$F_{O_3} = \varepsilon_{O_3} \sigma T_t^4 \quad (13c)$$

where T_t is the temperature at the top of the atmosphere and σ the Stefan-Boltzmann constant. The value obtained in this way is $\varepsilon_{O_3} = 0.008345$.

Augustsson and Ramanathan [14] found that the weak bands of CO_2 are responsible for only a small part of the greenhouse effect and that its importance rises with increasing temperatures. A percentage correction in the final temperature predictions of

the present model will be taken from their work. The effects of other greenhouse gases (N_2O, CH_4 and clorofluorcarbons) are included in the emissivity ε_{0_3}.

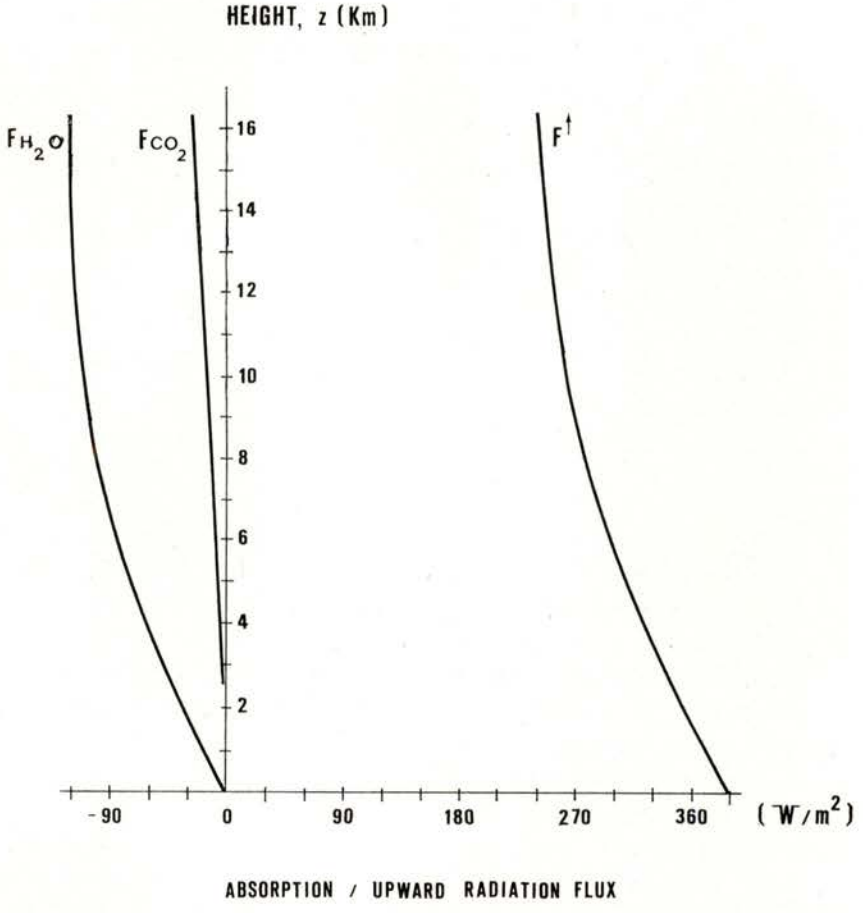

Fig. 7 — At left side, cumulative absorption of infrared radiation by H_2O and CO_2; at right, total upward infrared radiative flux in the atmosphere.

It is now important to stress that:

i) since the equations for the optical depth depend only on T(0), the total downward radiative flux (given by $S_0(1-\alpha)/4$, where S_0 is the solar constant, 1360 W/m²) is an (implicit) function of the superficial temperature;

ii) since absorber quantities and temperatures throughout atmosphere depend only of T(0), therefore the total infrared flux E is also a function of the superficial temperature. These facts are illustrated on Fig. 8, where one can see both fluxes as a function of T(0); as required, they are equal at the present globally averaged superficial temperature, 288 K.

The stability of this climatic system can be readily investigated through the equation that describes its energy balance,

$$dQ / dt = (S_0 / 4) \ (1 - \alpha) - E \tag{14a}$$

A small change $\delta T(0)$ in the superficial temperature gives:

$$\delta (dQ / dt) = [- (S_0 / 4) \ (d\alpha / dT(0)) - - (dE / dT(0)] \ \delta T(0) \tag{14b}$$

The numerical results indicate a value of -2.0 W / (m^2 K) for δ (dQ / dt), showing that the model is quite stable, fundamentally as a consequence of strong negative feedbacks introduced by the diffuse cloud. It is therefore not suprising that (see Fig. 9) the predicted rise in superficial temperature for, say, a duplication of current atmospheric CO_2 content is of only 0.7 K, or 0.8 K if one accounts for the weak bands.

The predicted changes in temperature are smaller than those predicted by other radiative convective models and by more complex tri-dimensional GCM's. A simple modification of the present model is to consider constant the amount of water in the cloud. This is equivalent to consider the fraction of condensed water remaining in the atmosphere at each level as a temperature-dependent function. In this way, the increase in superficial temperature for $2 \times Co_2$ levels is of 2.4 K. Note that in most models of the same type, modifications in cloudiness produce only insignificant effects.

In this final form, the model is assumed to represent well the atmospheric behaviour. The biospheric response to the modifications in temperature and precipitation shall now be considered.

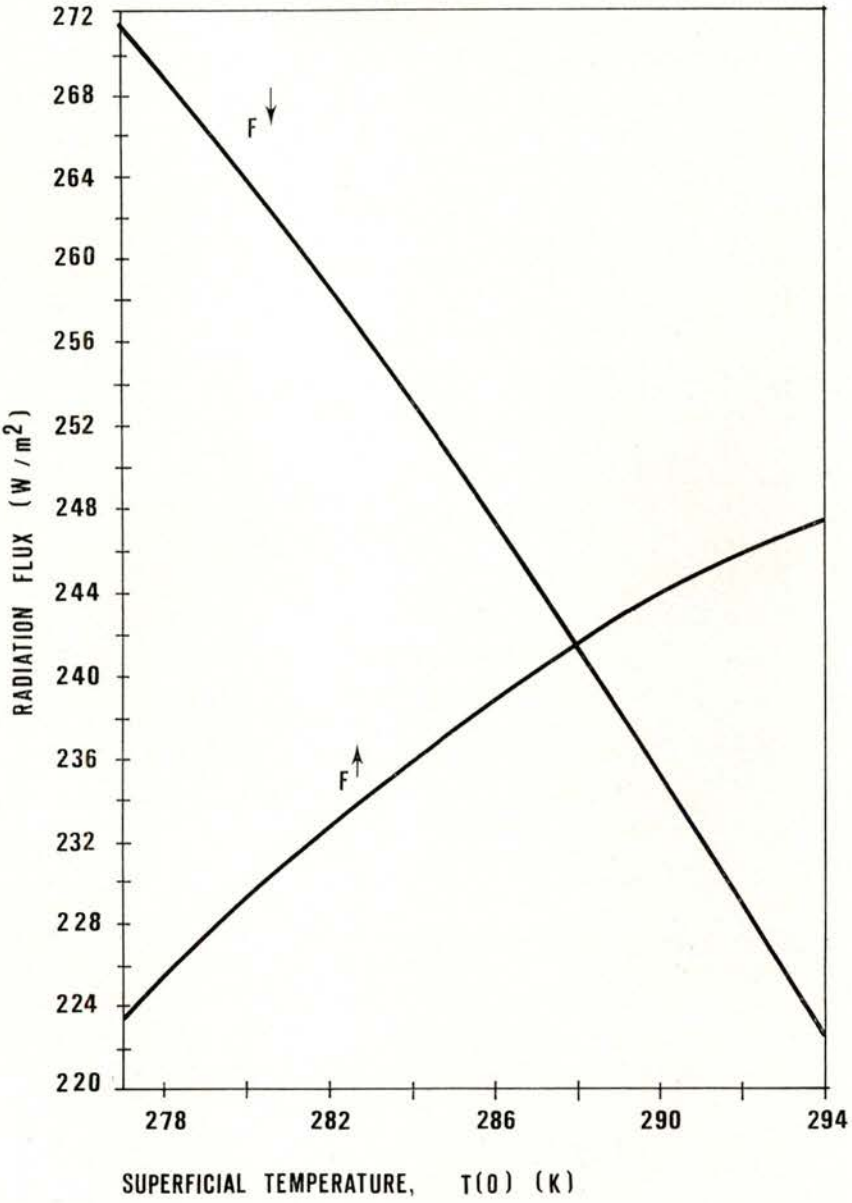

Fig. 8 — Upward and downward radiative fluxes in the atmosphere, as a function of superficial temperature.

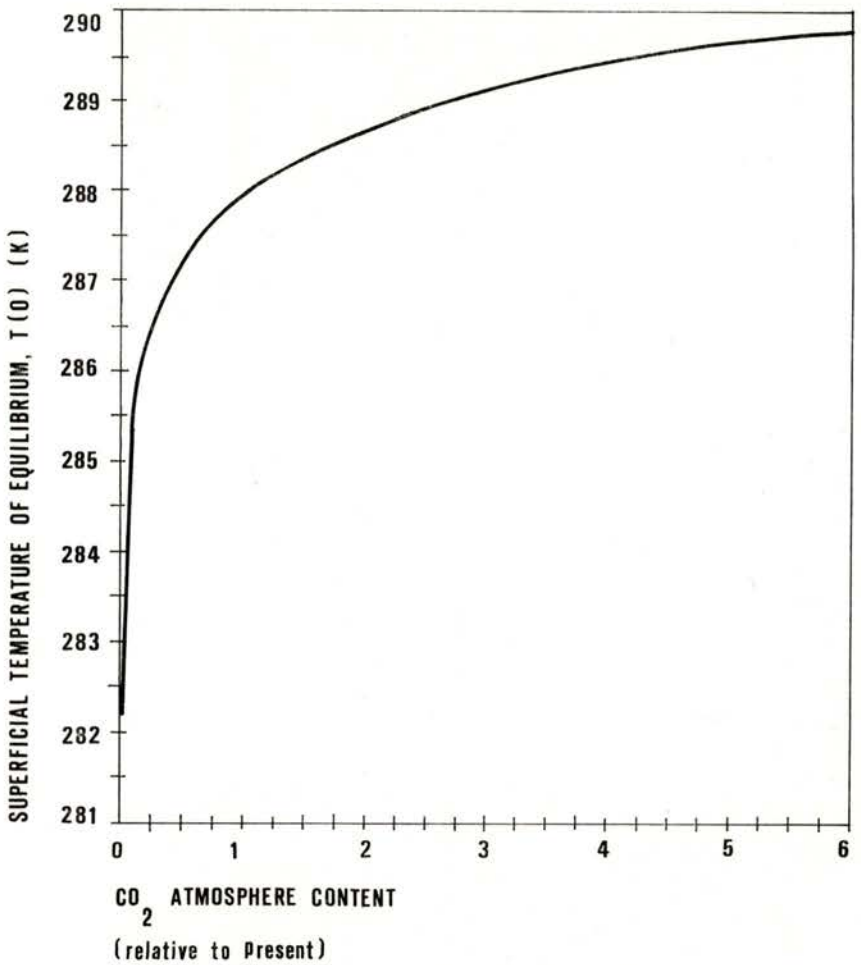

Fig. 9 — Evolution of superficial temperature as a function of CO_2 content of the atmosphere.

4 – MODELLING THE BIOSPHERIC RESPONSE

The use of a biozone classification system, depending on basic climatic indices only, was considered sufficient for the main purposes of this work, namely a preliminary impact assessment. With such a model it is possible to verify which are the changes in the boundary of the main biological-climatological regions,

resulting from the atmospheric and climatic modifications predicted by the two preceding sub-models; on this basis one can already produce (qualitative) impact estimates.

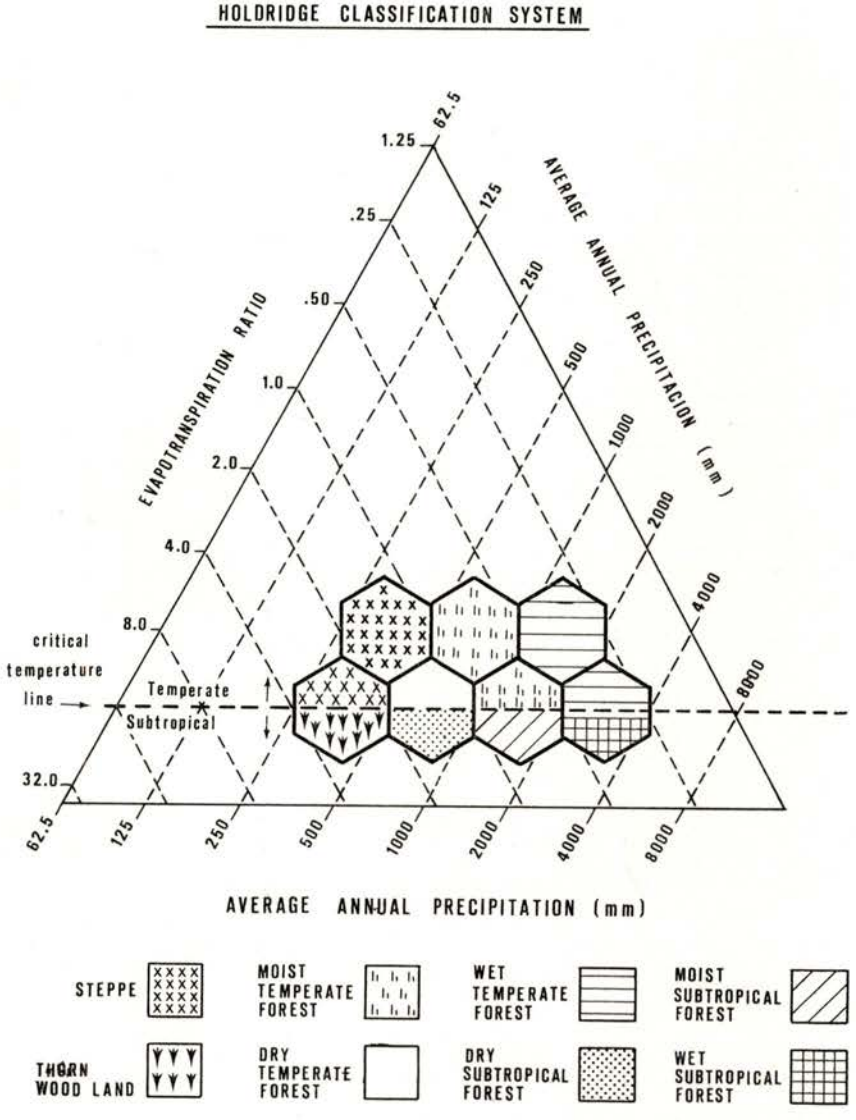

Fig. 10 — Holdridge Classification System; only some bioclimatic intervals are shown, the ones with pertinence for the present work.

The model selected is the Holdrige Bioclimatic Classification System [15] where the biozones are characterized only by annual averages of precipitation and temperature. The identification of the biozones can be made in a triangular diagram (see Fig. 10), where two sides of the triangle are precipitation axis and the left side is a potential evapotranspiration ratio axis, which is the ratio of potential evapotranspiration to annual average precipitation.

The potential evapotranspiration is defined to be equal to the quantity of water released by plants to the atmosphere, when the water available for plant growth is sufficient, but not excessive. Holdridge concluded, through the study of several ecosystems, that the average annual potential evapotranspiration can be considered proportional to the average annual biotemperature with a proporcionality constant of 58.93. The average annual biotemperature is calculated simply by setting all (monthly or daily) negative temperatures in the data to 0°C and averaging over the year.

A further subdivision of biozones results from the aplication of the criterium of existence of killing frost, due to its strong effects on the growth of plants. A critical temperature line at 18°C was assigned by Holdridge and divides Subtropical and Warm Temperate zones. However, this critical temperature can be regionally adjusted on the basis of information about real conditions.

5 — APPLYING THE THREE-COMPONENT MODEL: DISCUSSION AND RESULTS

With the sub-models discussed in sections 2., 3. and 4. for each aspect of the CO_2 problem one can finally evaluate a joint response of the earth-atmosphere-biosphere system to the man-made perturbation and apply it to the case of Portugal.

The time evolution of carbon levels in the atmosphere, under the predictions of the CO_2-cycle model and the expected evolutions of deforestation and fossil fuel consumption (Fig. 2) is introduced in the atmospheric model. For each CO_2 level, the steady-state superficial temperature is evaluated. Fig. 11 shows the time evolution of the increase in average superficial temperature. It is

seen that the temperature increase is not a linear function of carbon atmospheric levels since it slowers in time, due to the saturation of the CO_2 667 cm^{-1} absorption band. Duplication of carbon levels by the year 2080 yields an increase of 2.5 in average annual temperature.

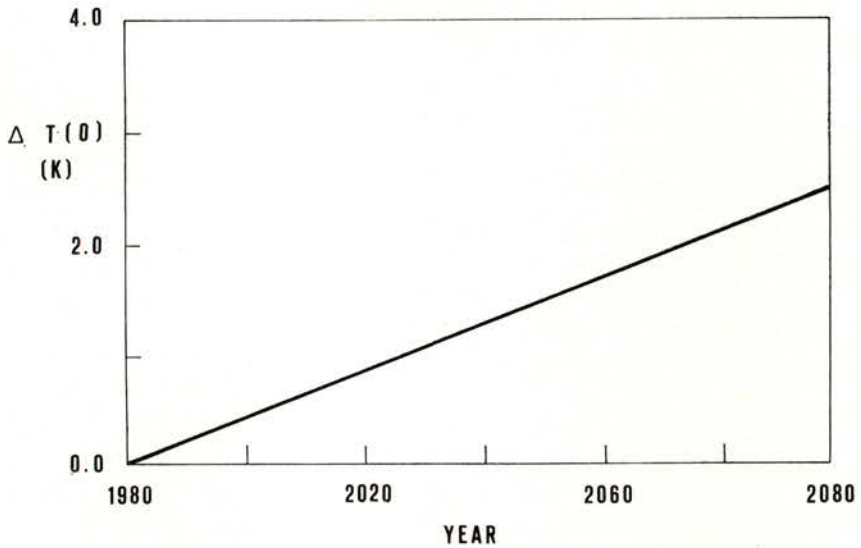

Fig. 11 — Time evolution of superficial annual average temperature, as computed from the CO_2 cycle and radiative-convective models.

An increment of 2 K seems therefore likely (in the present model, around year 2065) but the associated change in precipitation, that must also be provided for the bioclimatic model, is dubious. There are at present discrepancies between the numerical models that (as the present one) predict an increase in precipitation and some paleoclimatic analysis and empirical studies. From another point of view, the expected response of the atmosphere to higher CO_2 levels must be strongly regional-dependent, due to shiftings of the convective longitudinal cells. Indeed, the GCM's predict increments of superficial temperature for $2 \times CO_2$ levels higher than 5 K at polar regions and about only 1 K at equatorial regions. The reduced latitudinal temperature gradient induces weaker atmospheric movements, but evaporation and precipitable water would increase more than 6 %.

It is clear that one could employ the results of the radiative-convective model directly but, in view of the uncertainities explained above, it is felt that a comparative analysis can provide in this first study a better understanding of the bioclimatic response in Portugal. Therefore, when performing a comparison with average past conditions, two situations will be considered: an increment of 2 K in average annual temperature with i) an increment of 6 % in average annual precipitation in the «favourable» case; ii) a precipitation decrease of 6 % in the «unfavourable» case.

With climatological data from the 25-year period ranging from 1950 to 1975 [16], in locations providing a good coverage of the continental portuguese region, the Holdrige System was applied to yield a reference biozone distribution. This study is reflected on Fig. 12a and despite the substitution of natural vegetation, mainly by agricultural land and pine and eucalliptus forests, one can in fact see that the greater bioclimatic regions are well identified. It is speculated that consideration of seasonal precipitation oscillations and/or a finer data coverage could further separate the dryer southern and south-eastern regions from the more fertile regions of the west-atlantic coast and from the north-eastern mediterraneum micro-climates. The results yielded in the two case studies are shown in Figs. 12b and 12c.

The difference between the modified bioclimatic distributions and the reference distribution is considerable. By order of importance, the main modifications (which can be considered unfavorable from the agricultural and human point of view) are as follows:

i) substitution of the central and southern Warm Temperate Dry Woods for Subtropical Dry Wood,
ii) about a half-reduction in the Wet Mountain Forest located in the central-eastern region (around the Estrela mountain chain),
iii) appearance of a region of Subtropical Wood in the middle of the northern region.

It is important to notice that the difference between the favourable and unfavourable cases is not very important. Therefore, one can identify the average annual temperature as the decisive factor in a distribution of the bioclimatic regions in the continental Portuguese region. In fact, reduction of precipitation

instead of increment has its influence only in the moderate reduction of the nort-eastern low-mountain temperate dry woods and in

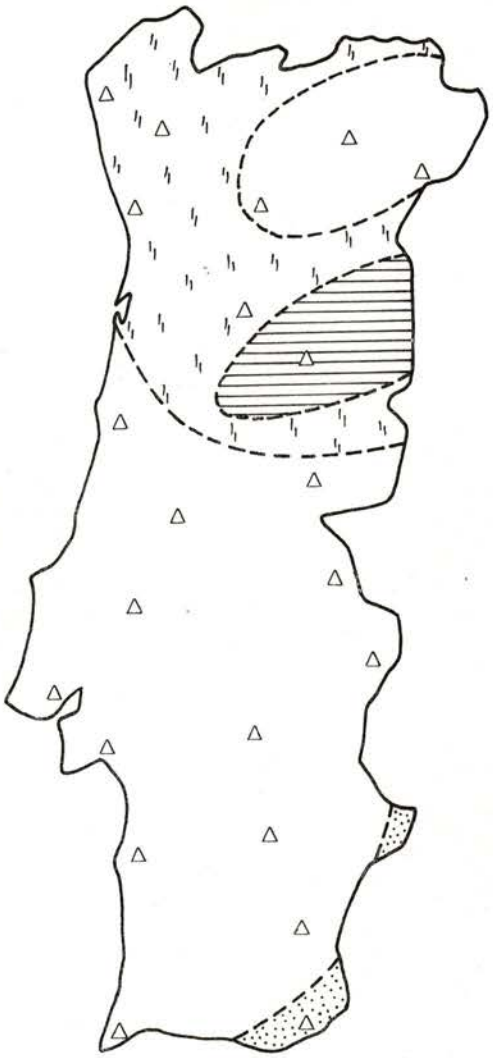

Fig. 12a — Reference bioclimatic distribution for Portugal, computed with climatological data from 1950 to 1975 observed in the locations indicated with triangles.

the appearance of small areas of dry subtropical woodlands. The latter effect indicates a desertification enhancement in those areas and nearby regions.

Fig. 12b — Same as Fig. 12a, but with an increase of 2 K in the annual biotemperature at each station and an increase of 6 % in the annual precipitation.

This first preliminary study indicates important potentially unfavourable consequences for the portuguese biosphere. It was also shown that the uncertainity in the precipitation has little

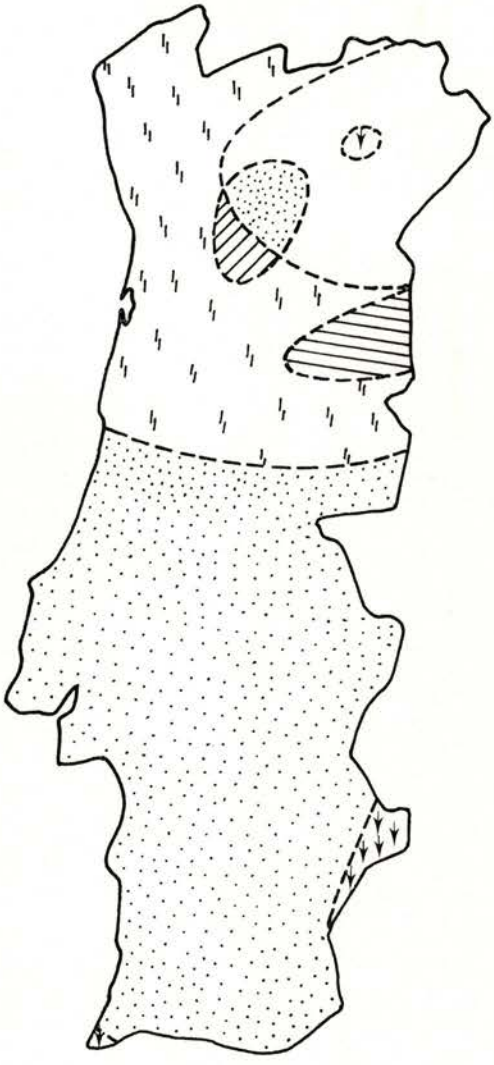

Fig. 12c — Same as Fig. 12b, but with a 6 % decrease in annual precipitation.

influence on the biozone distribution. Therefore, in further studies of CO_2 impact in the portuguese biosphere, the precipitation predicted by atmospheric models can be taken directly as input to biospheric models.

7 – CONCLUSIONS

A model that integrates the three main aspects of the CO_2 problem, namely the modelling of the carbon cycle, the atmospheric behaviour and the biosphere response was developed, calibrated and shown to be able to produce estimates of the time evolution of the earth-atmosphere-biosphere system. This model was applied to the case of Portugal and the results show that the temperature is the main factor influencing biozone distribution and that significative and potentially unfavourable changes in the portuguese bioclimatology are expected as a consequence of maninduced introduction of carbon dioxide in the atmosphere.

The present work can be extended along two directions:

i) using the fact that the described three-component model is simple and that the steady-state for each different set of boundary conditions is obtained from a single computation, it is possible to evaluate the transient response of the earth-atmosphere-biosphere system. In fact, feedbacks can be established among the various subcomponents: for instance, temperature-dependent absorption coefficients for the ocean take-up of carbon, and biospheric mass evolving with temperature, precipitation and CO_2 atmospheric levels.

ii) more detailed impact analysis of the climatologic changes predicted for the portuguese zone with GCM's can be made through the use of biospheric productivity models, yielding quantitative estimates for the modifications of the biosphere. Other aspects of the CO_2 problem as sea level rise, impact in specific agricultural species, or fisheries, must also receive attention, preferably through a sensitivity analysis in absence of reliable predictions for both long-term and seasonal meteorological and oceanic conditions under high CO_2 levels.

REFERENCES

[1] H. I. SCHIFF, A review of the carbon dioxide greenhouse problem. Plan. Space Sci., **29**, 935-950 (1981).

[2] R. J. AGUIAR, Efeitos Antropogénicos Sobre o Clima da Terra. Final-year Research Project, Lisbon University, F. C. L. (1985).

[3] R. AVENHAUS, S. FENYI and H. FRICK, Mathematical treatment of box models for the CO_2 cycle of earth. In «CO_2, Climate & Society» (1978).

[4] G. H. KHOLMAIER *et al.*, A non-linear interaction model between land biota and atmosphere. In «CO_2, Climate & Societè», J. Williams Ed., IIASA Series 1 (1978).

[5] B. C. WEARE and F. M. SNELL, A diffuse thin cloud atmospheric structure as a feedback mechanism in global climatic modelling. J. Atmos. Sci., **31**, 1725-1734 (1974).

[6] C. SAGAN and J. B. POLLACK, Anisotropic, nonconservative scattering and the clouds of Venus. J. Geophys. Res., **72**, 467-477 (1967).

[7] D. DEIRMENDJIAN, Scattering and polarization properties of water clouds and hazes in the visible and infrared. Appl. Opt., **3**, 187-196 (1964).

[8] S. TWOMEY and H. B. HOWELL, The relative merit of white and monocromathic light for the determination of visibility and backscattering measurements, Appl. Ppt., **4**, 501-506 (1965).

[9] J. T. HOLLIN, On the glacial history of Antartica, J. Glaciology **4**, 173-195 (1962).

[10] N. A. MORNER, Climatic changes during the last 35 000 years as indicated by land, sea and air data, Boreas, **2**, 34-53 (1973).

[11] C. D. RODGERS, The use of emissivity in atmospheric radiation calculations. Quart. J. R. Met. Soc. 43-54 (1966).

[12] C. D. RODGERS and C. D. WALSHAW, The computation of infrared cooling rate in planetary atmospheres, Quart. J. R. Met. Soc., **94**, 67-72 (1967).

[13] D. O. STALEY and G. M. JURICA, Flux emissivity tables for water vapour, carbon dioxide and ozone, J. Appl. Met., **11**, 241-254 (1970).

[14] T. AUGUSTSSON and V. RAMANATHAN, A radiative-convective study of the CO_2 climate problem, J. Atmos. Sci., **34**, 448-451 (1977).

[15] L. R. HOLDRIDGE, Determination of world plant formation from simple climatic data. Science, **105**, 367-368 (1947).

[16] Anuário Climatológico de Portugal, Instituto Nacional de Meteorologia e Geofísica, Lisbon, Portugal (1950 to 1975).